

Mapping the Vacuum Magnetic Surfaces in Heliac H-1NF Using Techniques in Tomography

TUMLOS Roy B., BLACKWELL Boyd D.¹ and HOWARD John¹

Plasma Physics Laboratory, National Institute of Physics

University of the Philippines, Diliman 1011 Quezon City, Philippines

¹*Plasma Research Laboratory, Australian National University, Canberra, Australia*

(Received: 30 September 1997/Accepted: 22 October 1997)

Abstract

A novel approach is used in studying the error fields in the heliac facility "H-1NF" in the Plasma Research Laboratory of the Australian National University by an electron beam mapping technique using a rotating multi-wire grid collector and a reconstruction technique developed in tomography known as Algebraic Reconstruction Technique (ART). Some error fields in H-1NF are identified by comparing maps of the vacuum magnetic surfaces from this technique with the maps generated from the HELIAC magnetic field tracing code. The results are compared with those of maps obtained using the fluorescent detector.

Keywords:

heliac, Poincaré plot, low energy electron beam, tomography, mapping, multi-wire grid, vacuum magnetic surface, error field, fluorescent detector

1. Introduction

In H-1NF [1], the sources of error fields due to coil positional errors and other peculiarities of its engineering design were studied before other major experiments were done. This is to confirm the accuracy of the construction and to insure that the magnetic model of H-1NF used by the computer code HELIAC [2] has adequate details of the machine, and that the magnetic configurations simulated using the code are as near to the reality in the H-1NF. There are two techniques, both using an electron beam, that are utilized for this end: the first uses a fluorescent detector [3] and the second uses a multi-wire grid collector [4, 5]. This paper will focus on the multi-wire grid technique.

2. Experimental Setup

The vacuum magnetic surface in H-1NF are mapped by a beam (~ 0.7 mm-dia) of low energy electrons (15–130 eV and ~ 1 μ A) using a multi-wire grid

collector consisting of 64 molybdenum wires (0.15 mm-dia) spaced at 4 mm. The electron gun is located at the toroidal angle 120° while the collector is located at 85° , shown in Figure 1. The collector is rotated by typically 0.6° angular steps and a total of 290 to 360 projections are made of a vacuum magnetic surface depending on its size. (See Figure 2 for the diagram of the collector.) The collector is permanently installed inside the vacuum vessel of H-1NF and can be parked away from the plasma.

For each scan step, the signal from the wires are sampled using a 64-channel multiplexer, allowing the use of a single instrumentation-quality isolation amplifier. Both the preamplifier and the active low-pass filter stages of the signal processing electronics use MOS ICs which have a very good noise immunity and very low quiescent current. An example of the raw data is shown in Figure 3a.

*Corresponding author's e-mail: troyb@nip.upd.edu.ph

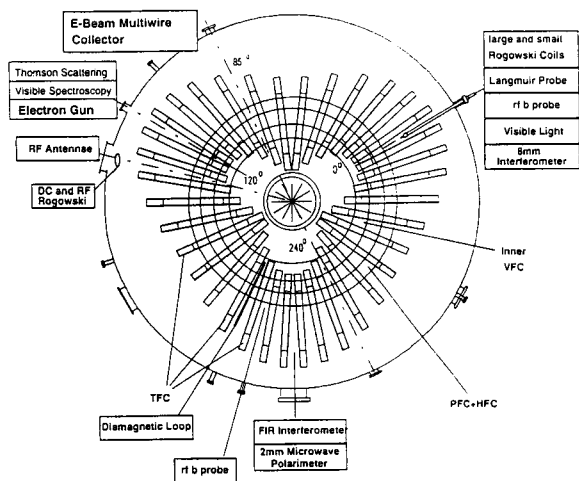


Fig. 1 Top view of the H-1 showing the locations of the different diagnostic systems. The multi-wire grid detector is at $\phi=85^\circ$ and the electron gun is at $\phi=120^\circ$.

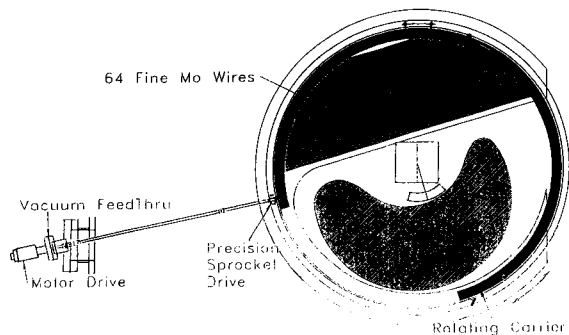


Fig. 2 The poloidal view of the e-beam detector in "park" position.

3. Reconstruction of the Data

The projection data of a vacuum magnetic surface can be quickly assessed by simply back-projecting it to the polar plane and then translating the identified beam centers into the H-1NF machine rectangular coordinates, as shown in the Figures 3(a)-(c). This approach is less time consuming and the result is readily compared to the Poincare plots from the HELIAC code.

Another way of producing the maps from the projection data is through an iterative method using ART[6]. This approach incorporates some *a priori* knowledge of the geometry of the detector and the vacuum magnetic surface to optimize the final image and increase the computational efficiency of the method. The method is adopted in the reconstruction because although the angular resolution of the wire grid

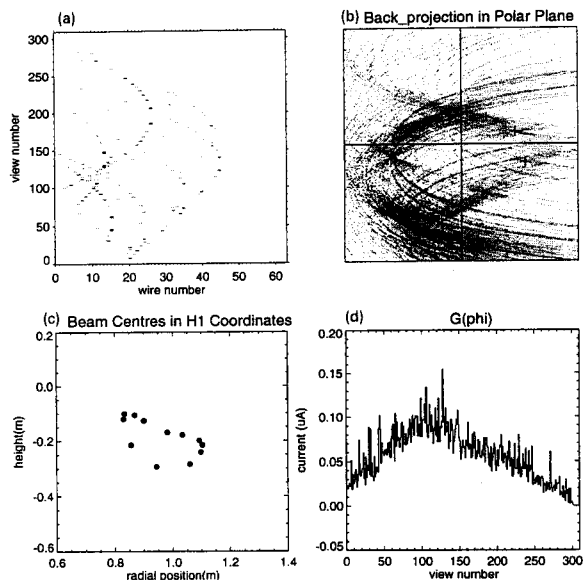


Fig. 3 Mapping a vacuum magnetic surface for the standard case. (a) Raw data. (b) Simple back-projection in polar plane. (c) Beam centres translated into H-1NF machine coordinates. (d) Net current in the detector.

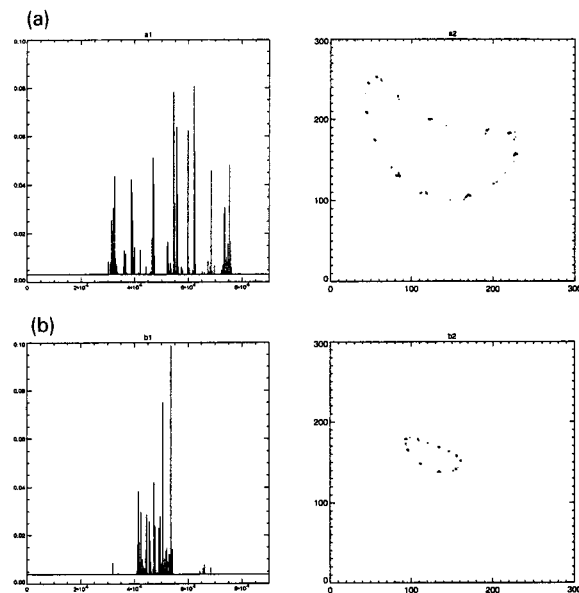


Fig. 4 Contour plots of (a) an outer surface and (b) an inner surface for the standard case processed using the multiplicative ART.

apparatus is adequate, the spatial resolution is not, *i.e.*, the wire separation is $\approx 4\times$ the beam width. Aside from this, the detector is also constrained (for mechanical reasons) so that some sections of the bigger magnetic surfaces receive only partial angular coverage. The

undersampling can readily be observed for the bigger surfaces as wing-like artifacts in the image, as shown in Figure 4[7].

4. Error Field Analysis Using the Maps

The maps from the experiment are compared to the HELIAC code generated Poincaré plots for agreement. Initially, the code already incorporated some of the known error field sources, e.g., some unavoidable positional errors in few individual TF coils. The vertical field and the toroidal field coils of H-1NF are calibrated to within a millimeter but the positional errors of the effective axis of the TFC set relative to the central conductors, (including the poloidal field coil (PFC) and the helical coil which can affect the up-down symmetry of the magnetic surface the most) and the field errors resulting from the cross-over in the coils are not known that accurately.

The H-1NF being a flexible heliac has the advantage over other stellarators in this case. There are many configurations that can be studied for error field analysis. Firstly, one can start with the standard configuration, when the helical field coil current is zero, $I_h = 0$. Maps for resonant values of rotational transform, such as $1/1$ and $5/4$, can be used to emphasize particular

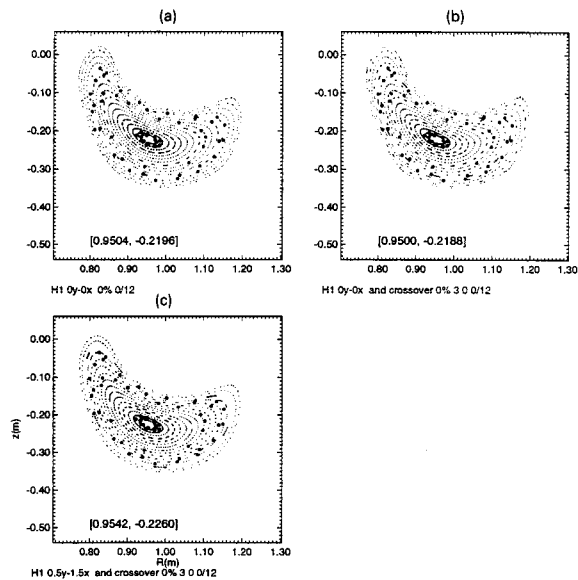


Fig. 5 Comparing the mapped magnetic surfaces of the standard case with the HELIAC code (a) with "ideal" case, (b) with only the PFC current cross-overs correction, and (c) with both cross-over corrections and the central ring conductor shifts. Shown in bracket is the magnetic axis position ($[R, z]$).

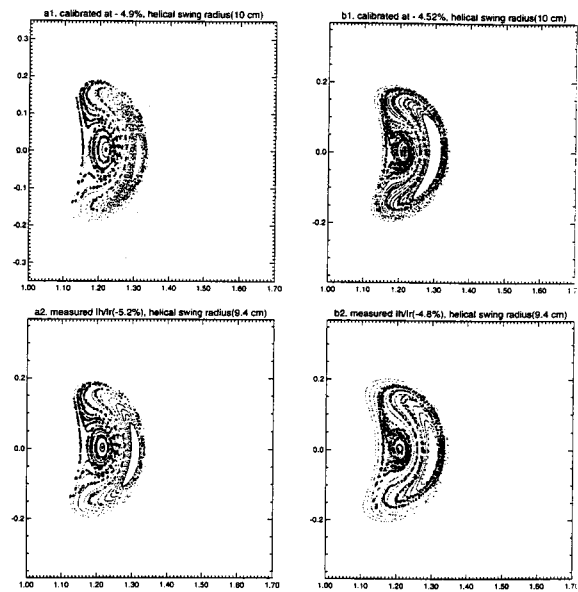


Fig. 6 Diagram of the central ring conductor displacement with respect to the toroidal coils.

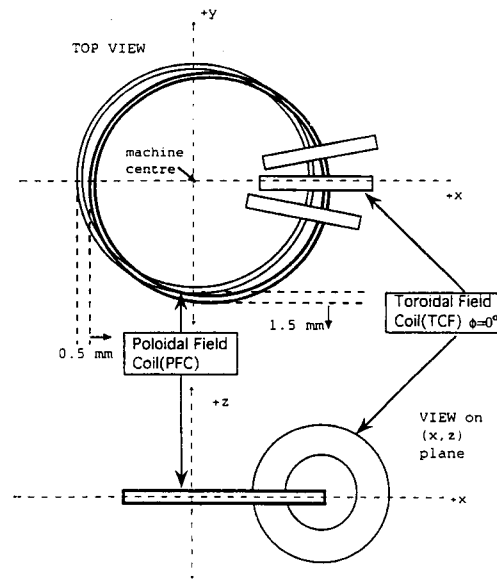


Fig. 7 Fluorescent technique maps of a $1/1$ island for calibrating the helical swing radius. The measured helical current, I_h/I_t , is -5.2% . In a1 the Heliac code is run at -4.9% helical current and at 10 cm helical swing radius to get a rough match while in a2, an almost exact match is achieved with a helical swing radius of 9.4 cm and using the measured I_h/I_t .

errors and refine initial analyses. As an illustration of these procedures, the standard case is used, shown in Figures 5(a)-(c), for comparing maps produced from the experiment and the code-generated Poincaré plots. Herein, it is concluded that the magnetic model, Figure 5c, must be corrected by shifting the central conductors position along the x -axis by -1.5 mm and along the y -axis by 0.5 mm, as shown in Figure 6. This is a smaller correction than previously inferred using the fluorescent detector maps: a displacement of -2 mm along the x -axis and 1.5 mm along the y -axis. With this, the $5/4$ resonance maps using the fluorescent detector are re-examined and shown to match when the code has the corrections in the central coil displacement and the correction in the current cross-overs, as shown in Figure 7. The swing radius of the helical conductor is also recalibrated from 10 cm to 9.4 cm using the procedure based on the comparison of the $1/1$ resonance maps, also using fluorescent detector, with the Poincaré plots, as shown in Figure 8.

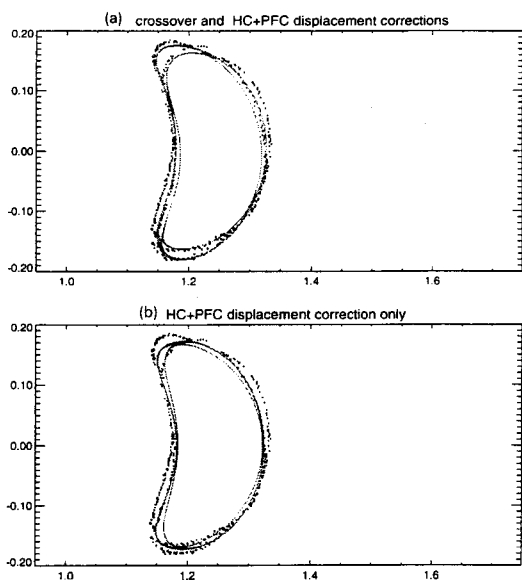


Fig. 8 Fluorescent technique map of a $5/4$ resonant island illustrating the critical nature of the current cross-overs to get a match with the Poincaré plot.

5. Conclusion

The multi-wire grid technique is in principle, a precise and high resolution method for mapping magnetic fields. These early results are a proof of principle, and show that it is an effective method for analyzing error fields. Several key error parameters of the H-1 coil set have been determined: the positional offset of central conductors and the helical core swing radius. Also, the role of the current cross-overs in the PFC as simulated in the HELIAC code is validated in the comparisons. The imaging potential of this technique is demonstrated, using a simple tomographic inversion method.

Acknowledgments

The authors would like to acknowledge the former head of the Plasma Research Laboratory (PRL), Prof. S. Hamberger for spearheading the establishment of the heliac facility H-1NF. We would also like to thank Dr. M. Shats, Dr. L. Sharp and Mr. D. Rudakov for their advice and the fluorescent mapping data. The first author would like to thank the Australian government through the Australian International Development Assistance Bureau (AIDAB) and the University of the Philippines for supporting his Ph. D. education in PRL.

References

- [1] G. G. Borg, B. D. Blackwell, S. M. Hamberger, D. L. Rudakov, D. A. Schneider, L. E. Sharp, M. G. Shats and B. C. Zhang, *Fusion Eng. and Design* **26**, 191 (1995).
- [2] A. B. Ehrhardt, *Helicac's User's Guide*, Princeton Plasma Physics Laboratory, Version 2 (1985).
- [3] M. G. Shats *et al.*, *Nucl. Fusion* **34**, 1653 (1994).
- [4] B. D. Blackwell, J. Howard and R. B. Tumlos, *Rev. Sci. Inst.* **63**, 4725 (1992).
- [5] R. B. Tumlos, Ph. D. Thesis, *Studies of Vacuum Magnetic Surfaces in H-1 Using Tomography*, Australian National University (1994).
- [6] G. T. Herman, *Image Reconstruction from Projections*, The Fundamentals of Computerized Tomography (Academic Press, New York, 1980).
- [7] J. Howard, *Journal of the Optical Society of America A* **5**, 999 (1988).